groove widths 0.603, $x_i^2 = 0.1455$, $x_s^2 = 0.6344$, $x_0^2 = 1.44$. The curves 1-5 correspond to Λ = 13.7, 41, 136, 957, and 1777; the broken lines correspond to the limiting solution on the smooth part. The curves 4 and 5 on this section are virtually identical with the limiting curve and are not shown in the figure.

As follows from (3.2), with h = const on the smooth part $p = \Lambda^{1/2}\left[\frac{\sin 2\alpha}{\mathrm{ch}^2 x_i^2}\left(\langle h\rangle - \frac{\langle h^{-2}\rangle}{\langle h^{-3}\rangle}\right)\Big|_{x^2=x_i^2}\right]^{1/2}\frac{\sqrt{x_0^2-x^2}}{h^{3/2}}$. One can see that the pressure and therefore also the carrying capacity are maximum for $\alpha = 45°$. It also follows from the formula that the pressure p reaches the maximum value p_{max} at $x^2 = x_s^2$.

Figure 4 shows the two dependences $p_{max}(\Lambda)$ (1: the reduced asymptotic solution; 2: the result of the computer solution of the complete problem).

We thank M. A. Galakhov for a discussion of some of the results of this work.

LITERATURE CITED

1. A. N. Burmistrov and V. P. Kovalev, "Asymptotic methods in the theory of lubrication: theoretical and experimental study of the motion of liquids and gases," in: Interdepartmental Symposium [in Russian], Moscow Physical Engineering Institute, Moscow (1985).
2. H. G. Elrod, "Thin-film lubrication theory for newtonian fluids with surface processing striated roughness or grooving," Trans. ASME Ser. F. J. Lubric. Technol., 95, No. 4 (1973).
3. Ya. M. Kotlyar, "Asymptotic solution of Reynolds equations," Izv. Akad. Nauk SSSR, MZhG, No. 5 (1976).
4. Julian D. Cole, Perturbation Methods in Applied Mathematics, Blaisdel Publishing Co., Toronto (1968).

STRUCTURE OF SHOCK WAVES IN POROUS IRON AT LOW PRESSURES

V. N. Aptukov, P. K. Nikolaev, and V. I. Romanchenko

UDC 539.374+624.131

The interest shown in the study of the behavior of porous materials under shock loading is due to their practical application in the explosive compaction of parts [1], their use in various types of shock-wave dampers [2], and the possibility such investigation offers for realizing a broad range of thermodynamic states in substances [3, 4].

The high-pressure region of shock compression, above 10 GPa, has traditionally been studied more intensively. This is due to the rapid strides made in shock-wave physics in recent years. In the low-pressure region – where the most important mechanical effects are realized in terms of the strength and plastic flow of a material in pores – relatively little information has been collected. The data that is available is restricted to isolated materials and porosities, and the results are often contradictory [2].

The well-known models of the mechanical behavior of porous materials fall into two groups: equilibrium models with an explicit $p \sim \rho$ relation [5, 6], and nonequilibrium models reflecting the kinetics of pore collapse [7-10].

Here, on the basis of the thermomechanical principles of a continuum with internal state parameters, we propose a model of the behavior of porous solids under shock loading. The results of mathematical modeling are compared with experimental measurements we made of the compression-wave profile in porous iron at different initial porosities (10-40%). The profiles were obtained by means of pressure gauges.

1. Description of the Model. The mechanics of deformable porous solids are based on several hypotheses, the most important of which are the hypothesis of continuity and the postulate of macroscopic definability [11].

Perm'. Translated from Zhurnal Prikladnoi Mekhaniki i Tekhnicheskoi Fiziki, No. 4, pp. 92-98, July-August, 1988. Original article submitted March 25, 1987.

 0021-8944/88/2904-0540$12.50

The general system of equations of the thermomechanical behavior of a damaged elastic medium has the form [12-14]

$$\frac{1}{\rho}\dot{\rho} + \operatorname{div}\mathbf{v} = 0, \quad \operatorname{div}\boldsymbol{\sigma} + \rho\mathbf{F} = \rho\dot{\mathbf{v}},$$
$$z = z(\boldsymbol{\sigma}, \Theta, \boldsymbol{\varepsilon}^p, \boldsymbol{\varepsilon}^N), \quad \boldsymbol{\varepsilon} = -\rho\partial z/\partial\boldsymbol{\sigma}, \ \eta = -\partial z/\partial\Theta, \tag{1.1}$$
$$\dot{\boldsymbol{\varepsilon}}^p = \boldsymbol{\Phi}(\boldsymbol{\sigma}, \Theta, \boldsymbol{\varepsilon}^p, \boldsymbol{\varepsilon}^N), \ \dot{\boldsymbol{\varepsilon}}^N = \boldsymbol{\Psi}(\boldsymbol{\sigma}, \Theta, \boldsymbol{\varepsilon}^p, \boldsymbol{\varepsilon}^N),$$
$$\Theta\rho\dot{\eta} = \nabla\cdot(\boldsymbol{\varkappa}\cdot\nabla\Theta) + r^*\rho - \rho\frac{\partial z}{\partial\boldsymbol{\varepsilon}^p}:\dot{\boldsymbol{\varepsilon}}^p - \rho\frac{\partial z}{\partial\boldsymbol{\varepsilon}^N}:\dot{\boldsymbol{\varepsilon}}^N, \ -\rho\frac{\partial z}{\partial\boldsymbol{\varepsilon}^p}:\dot{\boldsymbol{\varepsilon}}^p - \rho\frac{\partial z}{\partial\boldsymbol{\varepsilon}^N}:\dot{\boldsymbol{\varepsilon}}^N \geqslant 0,$$

where $\boldsymbol{\sigma}$, $\boldsymbol{\varepsilon}$, $\boldsymbol{\varepsilon}^p$, $\boldsymbol{\varepsilon}^N$ are the stress and strain tensors (for the total strain, viscoplastic strain, and the strain due to the damages); $\mathbf{v}$ and $\mathbf{F}$ are the vectors of velocity and the body forces; ρ is density; Θ is temperature; η is entropy; z is free enthalpy; r^* is the density of the internal heat sources; $\boldsymbol{\varkappa}$ is the matrix of the thermal conductivities.

To make practical use of system (1.1) in solving specific problems, it is necessary to specify the functions z, $\boldsymbol{\Phi}$, and $\boldsymbol{\Psi}$ and the initial and boundary conditions. The tensors $\boldsymbol{\varepsilon}^p$ and $\boldsymbol{\varepsilon}^N$ in system (1.1) have the significance of internal state parameters of the medium that are attributable to the viscoplastic strains of the matrix and the strains connected with the change in the damage to the body. Here, we will use system (1.1) to derive the governing relations of initially porous bodies.

We will examine a porous isotropic medium with a relative pore volume $V^N = \bar{V}^N/\bar{V}_0$ [$\bar{V}^N$ is the volume of pores in a certain small volume $\bar{V} = \bar{V}^N + \bar{V}^m$, $\bar{V}^m$ is the volume of the matrix, $\bar{V}_0 = (\bar{V})_{t=0}$]. We will define the mean density of the porous material as $\rho = \rho^m\bar{V}^m/\bar{V} = \rho^m V^m/(V^N + V^m)$, $V^m = \bar{V}^m/\bar{V}_0$, where ρ^m is the running density of the matrix. If $V^N \to 0$ during loading, then $\rho \to \rho^m$. At the initial moment of time, $V^N = V_0^N$, $V_0^m + V_0^N = 1$, so that $\rho_0 = \rho_0^m(1 - V_0^N)$, where ρ_0^m is the initial density of the matrix of the material (in the persent case, the density of the porous iron). The volumetric deformation from the change in porosity is connected with the relative volume of the pores as $\varepsilon^N = V^N - V_0^N$.

We will assume that the function z has a form similar to its form for a nonporous thermoelastoviscoplastic material [13], the only difference being that the parameters of the medium are dependent on the relative volume of pores V^N:

$$-\rho z = \frac{1}{2}\left(\frac{p^2}{K(\Theta, V^N)} + \frac{\mathbf{S}:\mathbf{S}}{2G(\Theta, V^N)}\right) + \rho c_\Theta'(\Theta, V^N)\Theta(\ln\Theta - 1) + 3\alpha(\Theta, V^N)\Theta p + \mathbf{S}:\mathbf{e}^p + 3p\varepsilon^N. \tag{1.2}$$

Here, $p = (1/3)\boldsymbol{\sigma}:\mathbf{I}$; $\mathbf{S} = \boldsymbol{\sigma} - p\mathbf{I}$; $\mathbf{I}$ is the unit tensor; $\mathbf{e}^p$ is the deviator of the tensor of the viscoplastic strains. In Eq. (1.2), the matrix of the porous material is assumed to be plastically incompressible $\boldsymbol{\varepsilon}^p = \mathbf{e}^p$. The last term characterizes the work done by the mean pressure on the volumetric deformation due to the change in porosity.

In accordance with the expression $\boldsymbol{\varepsilon} = -\rho\partial z/\partial\boldsymbol{\sigma}$ [see (1.1)], we can use (1.2) to obtain physical equations for the porous material:

$$\varepsilon = \frac{1}{3}\frac{p}{K(\Theta, V^N)} + \alpha(\Theta, V^N)\Theta + \varepsilon^N, \quad \mathbf{e} = \frac{1}{2}\frac{\mathbf{S}}{G(\Theta, V^N)} + \mathbf{e}^p. \tag{1.3}$$

Thus, the total strain of the material is determined by the volumetric elastic deformation of the matrix, the temperature, and the strain due to the change in relative pore volume.

Having inserted Eq. (1.2) into thermodynamic inequality (1.1) and assuming that the change in density is small, we have

$$\mathbf{S}:\dot{\mathbf{e}}^p + 3p'\dot{\varepsilon}^N \geqslant 0, \ p' = p - p^\mu; \tag{1.4}$$

$$p^\mu = -\frac{1}{2}\left(\frac{\partial K}{\partial V^N}\frac{p^2}{K^2} + \frac{1}{2}\frac{\partial G}{\partial V^N}\frac{\mathbf{S}:\mathbf{S}}{G^2}\right) - 3\Theta\frac{\partial\alpha'}{\partial V^N}p - \rho\frac{\partial c_\Theta'}{\partial V^N}\Theta(\ln\Theta - 1). \tag{1.5}$$

We take the following [15] for the form of the evolutionary equation for the viscoplastic strain

$$\dot{\mathbf{e}}^p = \Phi\left\langle\frac{\sigma_u}{\sigma_s} - 1\right\rangle\frac{\mathbf{S}}{\sigma_u}, \tag{1.6}$$

where $\Phi(\ldots) = \Phi(\langle\ldots\rangle > 0)$ $(0(\langle\ldots\rangle \leqslant 0))$; $\sigma_s = \sigma_s(\Theta, e_u^p, V^N)$ are the equilibrium yield point (dependent on temperature), the intensity of the plastic strains e_u^p, and porosity; σ_u is the intensity of the stresses. The evolutionary equation for the change in volumetric strain due to

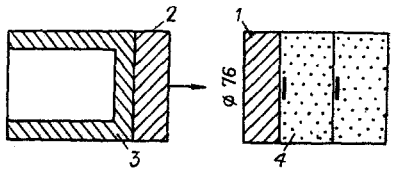

Fig. 1

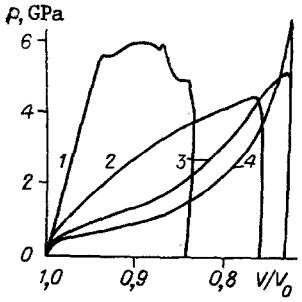

Fig. 2

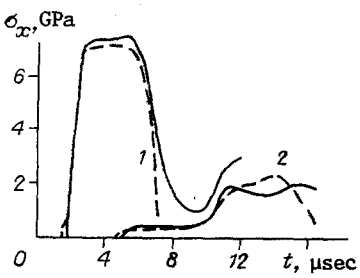

Fig. 3

porosity is formulated in a form similar to (1.6): $\dot{\varepsilon}^N = \Psi\langle p'/p^* - 1\rangle$ (p^* is a threshold parameter dependent on V^N and Θ).

To satisfy the thermodynamic inequality (1.4), it is necessary to satisfy the requirements $\Phi\langle\ldots\rangle \mathbf{S} : \mathbf{S}/\sigma_u + 3p'\Psi\langle\ldots\rangle \geqslant 0$. The inequality is satisfied by virtue of the definition of the function Φ, as well as under the conditions

$$\Psi\langle\ldots\rangle = \begin{cases} \Psi > 0, & \text{if} \quad p' > p_+^* > 0, \\ \Psi < 0, & \text{if} \quad p' < p_-^* < 0, \\ 0, & \text{if} \quad p_-^* \leqslant p' \leqslant p_+^*. \end{cases}$$

We obtain the equation for the change in temperature in an adiabatic approximation by means of (1.1) and (1.2): $\rho c_\Theta \dot{\Theta} = r^*\rho - 3\Theta\alpha\dot{p} + \mathbf{S} : \dot{\mathbf{e}}^p + (p' + \Theta\partial p^\mu/\partial\Theta)\dot{\varepsilon}^N$. Expressing p from Eq. (1.3) and differentiating over time, we find

$$\dot{p} = 3K(\dot{\varepsilon} - \alpha\dot{\Theta} - \dot{\varepsilon}^N) + 3\frac{\partial K}{\partial V^N}\dot{\varepsilon}^N(\varepsilon - \alpha\Theta - \varepsilon^N) \approx 3K(\dot{\varepsilon} - \alpha\dot{\Theta} - \dot{\varepsilon}^N).$$

The last relation reflects the phenomenon of loss of stiffness by the porous material with progressive pore collapse [2]. The mechanism of such collapse consists of intensive flow into the pores spaces (developed microplastic flow) with small macrostrains of the matrix. Thus, with only a small change in pressure, the volumetric deformation of the porous material is substantial due to an intensive change in porosity. In experimental p ~ ρ curves, this phenomenon corresponds to a sharp reduction in the slope of the adiabatic curve.

2. Description of the Experiment. Specimens were subjected to dynamic loading on a ballistic accelerator. The accelerator provided for plane collision of the surfaces of the striker and the target (Fig. 1). A steel plate 2 that was 10-12 mm thick was thrown against a steel shield 1 that was 8 mm thick. The plate was mounted on an aluminum striker 3 that was accelerated in the accelerator. Two of three disks of porous iron (powders of grade PZh4 M3) were placed behind the shield, while pressure gauges 4 were placed between the disks to record the profile of the transmitted shock wave. The measurement procedures used were similar to those employed in [16] for nonporous specimens. The experiments showed that a shock wave in porous iron has a two-wave configuration, similar to the elastoplastic case.

The low-amplitude wave propagates at a high velocity, which is evidently the result of the strength of the powder particles [17]. The pressure in the wave depends on the collision velocity. The first wave is followed by a second wave in which plastic flow of material into the pores occurs at a high rate. The pressure in the second wave rapidly decays with distance, so that the gauge records only the first wave when the collision velocity is low. Synchronous recording of pressure by two gauges at different points made it possible to measure the mean velocities of the first and the second waves through the thickness of the disks and the attenuation of the second wave during propagation.

Table 1 shows some of the results of measurement of the parameters of the shock waves in porous iron.

3. Results. Numerical calculations performed with allowance for temperature showed that the heating of the material with a low-intensity loading pulse is localized near the loading surface and has almost no effect on the decay of the compression wave. Thus, in the collision of a steel striker with a plate of porous iron (initial porosity 20%) at a velocity of 200 m/sec, the surface layer of the target is heated 40°C. At a collision velocity of 500 m/sec, it is heated 130°C. Thus, we will henceforth use the simplest variant of the model, not allowing for the heating of the material during shock compression. The numerical experiment corresponded to the conditions of the test: a steel striker-plate was collected

TABLE 1

Number of experiment	Initial velocity, m/sec	Initial porosity, V_0^N	Amplitude of pulse, GPa		Difference between theoretical and experimental data, %		Velocity of waves, km/sec		Difference between theoretical and experimental data, %	
			gauge 1	gauge 2	gauge 1	gauge 2	first wave	second wave	first wave	second wave
1	145	0,1	1,50	0,625 *	10	3,2	5,08	—	2,4	—
2	239	0,1	2,50	0,625 *	6	3,2	5,08	—	6,6	—
3	644	0,1	9,05	6,7	0	13,9	5,08	2,69	3,1	3,2
4	163	0,2	1,1	0,37 *	1,6	10,2	4,4	—	3,2	—
5	642	0,2	7,5	1,9	2,7	13,1	4	1,55	3,0	2,7
6	635	0,3	5,6	1,65	3,7	11,8	3,95	1,27	4,4	1,5
7	486	0,4	3,25	0,8	9,4	2,5	2,9	0,85	14,4	4,3

*Only the first wave was recorded.

with a laminated target plate consisting of a thin surface layer and porous iron.

The function Ψ, determining the kinetics of pore collapse, was assigned in the form $\dot{\varepsilon}^N = \Psi \equiv \frac{V^N}{\tau}\left(\frac{p'}{p^*} - 1\right)^n$ (τ and n are parameters of the model). The dependence of the barrier pressure p^* on the running porosity V^N was taken in its form in [9], satisfactorily describing the static test data: $p^* = \sigma_s^0 \ln V^N/3$. The effect of the level of porosity V^N on the moduli K and G was approximated by the relations $K = K_0(1 - V^N)^k$, $G = G_0(1 - V^N)^m$.

The function Φ in the evolutionary equation for the viscoplastic strain of the matrix (1.5) was chosen on the basis of well-known data on the viscosity of metals at high strain rates, in combination with the method used in [14]. Thus, in the given formulation of the model, allowing for porosity and the kinetics of its change leads to the appearance of four additional constants: τ, n, k, m. The model parameters τ and n are chosen upon comparison of calculations and experiments according to the attenuation of the wave amplitude, the residual porosity of the tested specimens, and the time dependence of the pressure or masss speed on the various distances from the loading surface. The model parameters k and m are chosen on condition of agrement of the theoretical and experimental velocities of the body and shear waves in the porous material.

Calculations performed with different parameters τ and n showed that the model qualitatively describes the behavior of different porous media. Figure 2 shows how the parameter n affects the theoretical compression curve of the porous material ($V_0^N = 0.3$). Curves 1-4 correspond to n = 0.5, 1, 2, and 3. At $n \leqslant 1$, the theoretical $p \sim V$ curves are similar to the analogous empirical relations for soils and bulk materials, while at $n > 1$ they correspond to plastic flow into pores in porous materials.

Figures 3 and 4 illustrate the experimental (dashed lines) and theoretical (solid lines) stress profiles corresponding to gauges 1 and 2 (see Fig. 1) for test 5 (see Table 1). The model parameters n = 2, τ = 4 μsec, k = 2, and m = 4 were obtained from the best agreement between the theoretical and experimental curves. All of the remaining experiments were set up with unchanged model parameters and resulted in satisfactory agreement (Fig. 4 for test 2).

The experiment shows that the amplitude of the compression waves decays rapidly during propagation in the porous iron. Even with relatively low amplitudes, the plastic wave has a shock front. This is attributable to the characteristic form of the theoretical curves of shock compression $p \sim \rho_0^m(1 - V^N)$ shown in Fig. 5 (curves 1-4 correspond to $V_0^N = 0.4$, 0.3, 0.2, 0.1). The nonequilibrium nature of the process is manifest here in the absence of a single $p \sim \rho$ curve. The density of the material being compressed depends on factors other than just pressure: the mechanism of decay of the pulse is controlled to a considerable extent by the ratio of the velocities of the loading and unloading waves, which are determined by the running value of porosity and the kinetics of its change. We should also point out the appreciably nonlinear dependence of the velocity of the plastic wave on the amplitude of the compression pulse. With a reduction in the amplitude of the plastic wave to the elastic value, its velocity decreases to almost zero.

Figure 6 shows the decay of the amplitude of the shock waves (solid lines) and the distribution of residual porosity (dashed lines) through the thickness of a specimen of porous iron ($V_0^N = 0.2$) at collision velocities of 200, 400, and 600 m/sec (curves 1-3). Most of

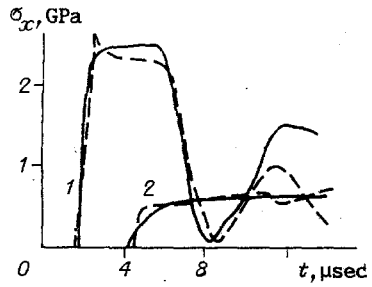

Fig. 4

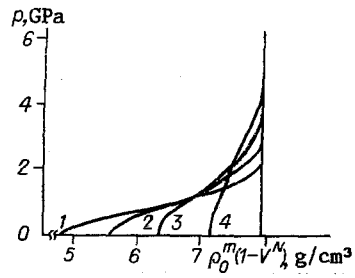

Fig. 5

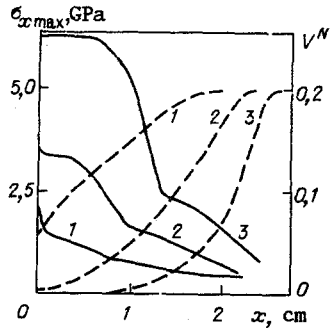

Fig. 6

the energy is expended on compaction of the front part of the plate. Only elastic waves or waves of low amplitude reach the rear region, and these waves do not lead to a significant reduction in porosity. In other words, a porous specimen is loaded considerably more nonuniformly by a shock wave than is a solid specimen.

Table 1 shows the difference between the experimental and theoretical amplitudes and velocities of the waves. We should point out the satisfactory agreement of the wave amplitudes obtained theoretically and experimentally from gauges 1 and 2. The differences in the velocity and form of the elastic precursor are evidently connected with the fact that we did not allow for the elastic change in porosity.

LITERATURE CITED

1. O. V. Romanov, V. F. Nesterenko, and I. M. Pikus, "Effect of the size of powder particles on the process of explosive pressing," Fiz. Goreniya Vzryva, No. 5 (1979).
2. V. Harriman, "Governing equations of porous materials undergoing compaction," in: Problems of the Theory of Plasticity/Mechanics. New Developments in Foreign Science [Russian translation], Vol. 7, Mir, Moscow (1976).
3. Ya. B. Zel'dovich and Yu. P. Raizer, Physics of Shock Waves and High-Temperature Hydrodynamic Phenomena [in Russian], Nauka, Moscow (1966).
4. S. B. Kormer, A. I. Funtikov, et al., "Dynamic compression of porous metals," Zh. Éksp. Teor. Fiz., 42, No. 3 (1962).
5. S. S. Grigoryan, "Basic concepts of soil dynamics," Prikl. Mat. Mekh., 24, No. 6 (1960).
6. S. Z. Dunin, V. K. Sirotkin, and V. V. Surkov, "Propagation of plastic waves in porous bodies," Izv. Akad. Nauk SSSR, Mekh. Tverd. Tela, No. 3 (1978).
7. G. M. Lyakhov, Waves in Soils and Porous Multicomponent Media [in Russian], Nauka, Moscow (1982).
8. R. I. Nigmatulin, Principles of the Mechanics of Heterogeneous Media [in Russian], Nauka, Moscow (1982).
9. A. F. Ovchinnikov, V. I. Pusev, and A. P. Gusarov, "Behavior of porous metals during compaction," in: Mechanics of Impulsive Processes [in Russian], MVTU, Moscow (1983).
10. M. M. Carrol and A. C. Holt, "State and dynamic pore-collapse relations for ductile porous materials," J. Appl. Phys., 43, No. 4 (1972).
11. A. A. Il'yushin, Continuum Mechanics [in Russian], Izd. MGU, Moscow (1978).
12. V. N. Aptukov, "Governing equation of the thermoelastic behavior and fracture of solids with small strains," in: Thermodynamics of the Deformation and Fracture of Solids with Microcracks [in Russian], UNTs (Ural Science Center) AN SSSR, Sverdlovsk (1982).
13. V. N. Aptukov and T. I. Kligman, "Nonlinear effects of an elastic medium with damages," in: Boundary-Value Problems of Elastic and Inelastic Systems [in Russian], UNTs AN SSSR, Sverdlovsk (1985).
14. V. N. Aptukov, "Model of a damaged thermoelastoviscoplastic medium: application to cleavage fracture," Fiz. Goreniya Vzryva, No. 2 (1986).
15. W. Nowacki, Wave Problems of the Theory of Plasticity [Russian translation], Mir, Moscow (1978).
16. V. I. Romanchenko and G. V. Stepanov, "Dependence of critical stresses on time-dependent load parameters in the cleavage of copper, aluminum, and steel," Zh. Prikl. Mekh. Tekh. Fiz., No. 4 (1980).
17. A. M. Staver, V. M. Fomin, and P. A. Cheskidov, "Structure of strong shock waves in powders," Transactions of the VIII All-Union Conference on Numerical Methods of Solving Problems of the Theory of Elasticity and Plasticity, ITPM SO AN SSSR (Institute of Theoretical and Applied Mechanics, Siberian Branch, Academy of Sciences of the USSR), Novosibirsk (1984).